Bulletin of the New Zealand Society for Earthquake Engineering, Vol. 59, No. 3, September 2026

INFLUENCE OF GUSSET PLATE DESIGN ON THE COLLAPSE RISK OF BUCKLING-RESTRAINED BRACED FRAME BUILDINGS

S. Sistla[1], R. Chandramohan[2] and T.J. Sullivan[3]

(Submitted *July 2025*; Reviewed *November 2025*; Accepted *April 2026*)

ABSTRACT

This study examines the impact of gusset plate design on the collapse risk of two buckling-restrained braced frame (BRBF) buildings, incorporating superX and diagonal brace configurations. Nonlinear dynamic analysis shows that the gusset plate axial compressive strength is, on average, 30 % lower than the design strength estimated by NZS-3404, indicating that the current design approach may be non-conservative. This study explores three alternative design methods: *(i)* NZS-3404 design with modifications (NZS-3404-revised), *(ii)* Court-Patience (CP) method, and *(iii)* Notional load yield line (NLYL) method. On average, the gusset plate axial compressive strength obtained from dynamic analysis aligns closely with the design strengths predicted by the NZS-3404-revised and CP methods. The NLYL method explicitly accounts for the reduced strength of mid-span gusset plates in super-X and chevron-configured BRBFs. The gusset plate strengths from dynamic analysis are approximately 30 % greater than those estimated by the NLYL method, demonstrating that this approach is sufficiently conservative and therefore recommended for design. Within the limited range of brace and gusset plate configurations studied, the collapse risk is reduced by a factor of 3.5 when the NLYL method is used instead of the NZS-3404 method.

https://doi.org/10.5459/bnzsee.1766

INTRODUCTION

Buckling-restrained braces (BRBs) can resist both tensile and compressive forces with high ductility, making them more efficient than traditional concentric bracing systems [1]. Ensuring the stability of buckling-restrained brace (BRB) gusset plates and end zones against out-of-plane buckling is crucial for maintaining the structural integrity of BRB systems subjected to earthquakes. The current design practice for BRB gusset plate stability, as outlined in ANSI/AISC 341-22 [2], involves designing them to resist the peak brace axial force anticipated at the lower of 2 % or twice the peak drift corresponding to the design intensity level. This is achieved by using the column buckling curve and idealising gusset plates as equivalent struts with an effective length factor (k) of 0.7. Previous experimental studies have indicated that gusset plates may be undersized using this approach, resulting in premature out-of-plane buckling of gusset plates before the BRBs reach their full compression load-carrying capacity [e.g., 3–5].

Experimental investigations by Vazquez-Colunga *et al.* [3] showed up to a 15 % reduction in the axial strength of gusset plates under bidirectional loading compared to unidirectional loading. Khoo *et al.* [6] demonstrated that achieving satisfactory performance of BRBs without gusset plate buckling is possible under bidirectional loading conditions when the gusset plates are adequately sized. Court-Patience and Garnich [7] reported no significant influence of bidirectional loading on gusset plate strength estimated through sub-assembly tests and 3D continuum finite element simulations. A previous study conducted by Sistla *et al.* [8] also reported no significant influence of bidirectional loading on gusset plate performance and the collapse risk of a 4-storey superX configured steel BRBF building.

Previous studies [e.g., 3,4,7] have developed experimentally validated 3D continuum finite element models of BRB systems. Although these models are accurate and useful in understanding the stability of BRB systems at a sub-assembly level, they are computationally expensive for examining the global seismic performance of BRBF buildings. This study addresses the aforementioned research gaps by investigating the influence of gusset plate design on the collapse risk of two BRBF buildings with superX and diagonal brace configurations, designed in accordance with current New Zealand practice. The gusset plates will first be designed according to the NZS-3404 method, and subsequently, alternative methods proposed in the literature will be used to refine their design. A computationally efficient global BRBF numerical modelling approach, developed by Sistla *et al.* [8], will be employed to model superX and diagonally configured BRBF buildings with varying gusset plate designs. This modelling approach is capable of simulating the out-of-plane buckling failure in BRB gusset plates and end zones. Nonlinear dynamic analyses are conducted using these building models to address the following research questions:

- Can the current NZS-3404 gusset plate design approach mitigate gusset plate buckling in BRBF structures?
- Does the out-of-plane buckling failure mode of BRBs depend on the brace configuration and the gusset plate location (i.e. mid-span vs. corner gusset plates)?
- What potential design alternatives exist to minimise the impact of gusset plate buckling on the collapse risk of BRBF buildings?

[1] *Corresponding Author, Structural Engineer-Quoin Structural Consultants, Christchurch, New Zealand, saiteja802@gmail.com*
[2] *Senior Lecturer, University of Canterbury, Christchurch, New Zealand (Member)*
[3] *Professor, University of Canterbury, Christchurch, New Zealand (Fellow)*

GUSSET PLATE DESIGN METHODS

There are several stability assessment methods in the literature that consider gusset plates as either equivalent columns, plates, or column systems. The most common assessment method involves idealising a gusset plate as an equivalent column with an effective width and length calculated based on the method proposed by Thornton [9], as illustrated in Figure 1. Thornton suggested a dispersion angle of 30° to compute the effective width (b_w) of the gusset plate, as shown in Equation 1a. The parameters b and h required to compute b_w are shown in Figure 1. The effective length (l_w) is calculated as the average of L_1, L_2, and L_3. The nominal section capacity of the gusset plate ($N_{NZS-3404}$) according to NZS-3404 is evaluated using Equation 1b.

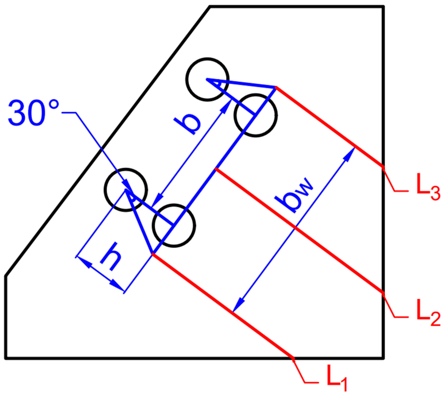

Figure 1: Equivalent column approximation of a gusset plate according to Thornton [9].

$$b_w = 2h\tan(30^\circ) + b \tag{1a}$$

$$N_{NZS-3404} = b_w t_g f_y \tag{1b}$$

$$P_{NZS-3404} = \alpha_c N_{NZS-3404} \tag{1c}$$

An effective length factor (k) of 0.7, thickness of the gusset plate (t_g), yield strength of the gusset plate (f_y), and l_w are used to compute the member slenderness factor (α_c), following the steps in Section 6.3.3 of NZS-3404. The critical gusset plate load ($P_{NZS-3404}$) is then estimated using Equation 1c. An example calculation for estimating the gusset plate capacity using the NZS-3404 method can be found in the Appendix section of [4]. The study conducted by Westeneng [4] compared the gusset plate design strength obtained by the NZS-3404 method to the gusset plate axial compressive strength obtained from two experimentally tested BRBFs that failed by gusset plate sway buckling. The NZS-3404 design method was found to be non-conservative in both cases. Although the NZS-3404 design method is similar to the AISC-341 [10] method, the AISC method uses a k value of 1.2 for gusset plates with free edges and 0.7 for gusset plates with stiffeners. To test the validity of the k values used in the AISC code, Chou *et al.* [11] conducted experiments on a 1-storey 1-bay steel BRBF. Their research recommends a k value of 2 instead of 1.2 for gusset plates with free edges. More recently, an experimental study conducted by Dong [12] on glulam frames with BRBs employed a k value of 2 in the gusset plate design, and no out-of-plane buckling failure was observed up to a drift ratio of 2 %. Therefore, the NZS-3404 gusset plate design method, modified by adopting a k value of 2 instead of 0.7 and referred to as the NZS-3404-revised method, is employed in this study as one of the alternative approaches for mitigating BRB gusset plate buckling.

A recent study conducted by Court-Patience and Garnich [7] assessed the stability of 184 gusset plates with varying brace angles, gusset plate slenderness, and gusset shapes (tapered vs. non-tapered). This was achieved by subjecting experimentally validated 3D continuum BRB sub-assembly models to unidirectional and bidirectional loading. A simple method to assess gusset plate stability was proposed based on the results obtained from these simulations. Their method, named the Court-Patience (CP) method, predicted the critical gusset plate buckling load over a range of slenderness ratio values with reasonable conservatism. The expressions to evaluate the critical gusset plate buckling load using the CP method are shown in Equations 2a to 2d.

$$N_{CP} = 1.2\, b_{w-15}\, t_g\, f_y \tag{2a}$$

$$\Lambda = \frac{(0.8L_2)k}{\pi r}\sqrt{\frac{f_y}{E}} \tag{2b}$$

$$P_{CP} = (0.658)^{\Lambda^2} N_{CP} \quad \text{if } \Lambda \leq 1.5 \tag{2c}$$

$$P_{CP} = (-0.06\Lambda + 0.68)N_{CP} \quad \text{if } \Lambda > 1.5 \tag{2d}$$

The section axial capacity under yielding, N_{CP}, is evaluated using Equation 2a. The effective gusset plate width in the CP method (b_{w-15}) is also estimated using Thornton's method, but with a dispersion angle of 15° instead of 30°. The slenderness parameter of the gusset plate is calculated using Equation 2b, where E is the Young's modulus and r is the radius of gyration, calculated as $t_g/\sqrt{12}$. In this approach, the effective length is taken as $0.8L_2$, as opposed to the average of L_1, L_2, and L_3 in the original Thornton method (Figure 1). A k value of 1.2 is adopted in this method, in contrast to the value of 0.7 specified in the NZS-3404 method. The value of N_{CP} is then reduced based on the slenderness parameter Λ (Equation 2b) to determine the critical gusset plate axial load, P_{CP}, as shown in Equations 2c and 2d.

The above-discussed methods do not explicitly account for bidirectional loading on gusset plates and the location of gusset plates within the BRBF, i.e., mid-span vs. corner. Zaboli *et al.* [13] developed the notional load yield line method (NLYL) for assessing the stability limit of mid-span and corner gusset plates, considering the BRB and gusset plate geometric imperfections and an out-of-plane drift of 1.2 %. This approach utilises a dispersion angle of 40° to estimate the yield capacity of the corner plates, while the yield capacity of the mid-span gusset plates is estimated using a dispersion angle of 30°. They have proposed stability equations based on symmetric, asymmetric (Figure 2), and one-sided collapse mechanisms. Their study demonstrated that the asymmetric buckling mode requires the least energy and is, therefore, the only mechanism considered in the present study. The stability equation for an asymmetric failure under the yield line of the gusset plates is shown in Equation 3a. Failure under the yield line results from hinging in the gusset plate, while failure above the yield line is due to hinging in the brace end zones. The BRBs in the present study are designed with stocky BRB end zones, and hinging is expected in the gusset plates. Hence, the asymmetric failure under the yield line is only considered. It should be noted that the commentary to the latest edition of the American steel design standard [2] encourages designers to adopt the NLYL method.

$$N_{ax}\Delta(\theta_1 + \theta_2)\delta_s \leq M_p^{gp}(2\theta_1 + \theta_2) \tag{3a}$$

$$\delta_s = \frac{1}{1 - \dfrac{N_{ax}}{N_{cr}}} \tag{3b}$$

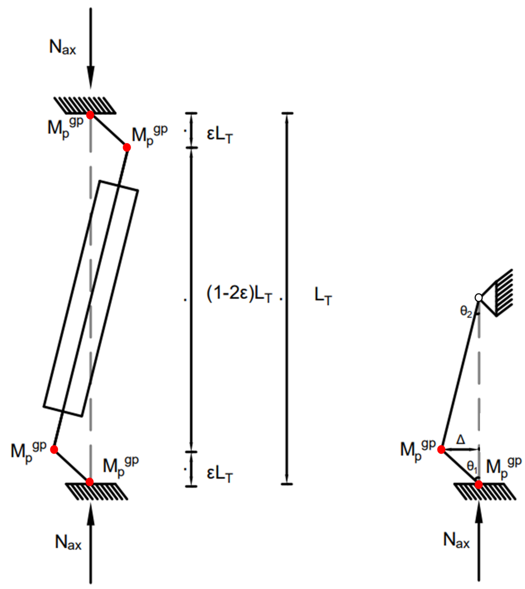

Figure 2: Asymmetric out-of-plane BRB failure mode under the gusset plate yield line according to the NLYL method.

In Equation 3a, N_{ax} is the axial load demand on the gusset plates (peak brace axial compressive force), Δ is the horizontal out-of-plane deflection of the gusset plate due to initial imperfection and out-of-plane drift (Figure 2), θ_1 is the rotation of the gusset plate, θ_2 is the rotation at the centre of the BRB, δ_s is the second-order moment amplification factor, and M_p^{gp} is the plastic moment capacity of the gusset plate. δ_s is calculated using Equation 3b, where N_{cr} is the critical buckling load of the BRB core-restrainer assembly. Equations to calculate Δ, M_p^{gp}, and N_{cr}, along with additional details and an example calculation for estimating the gusset plate capacity using the NLYL method, can be found in [13].

A key point to note is that effective length methods, such as the NZS 3404 method, cannot account for the influence of out-of-plane imperfections. In practice, if the imperfections exceed the prescribed limits, they can induce bending moments across the gusset plate's folding line, and the section can plastify. In such cases, the elastic buckling capacity of the plate can be significantly reduced. This is not an issue with the NLYL method, as it explicitly accounts for imperfections.

In the subsequent sections, besides the NZS-3404 method, three other methods discussed in this section will be considered for comparison. These three alternatives to the NZS-3404 method were selected due to their ease of application in practical scenarios. Readers interested in various other methods are directed towards Westeneng [4], Vazquez-Colunga *et al.* [3], Song *et al.* [5], and Takeuchi *et al.* [14].

DESIGN OF THE CASE-STUDY BRBF BUILDINGS

Two hypothetical 4-storey steel BRBF buildings (illustrated in Figure 3) are assumed to be located in Christchurch, on soil type D. Both buildings have a similar square floor plan with dimensions of 28 m × 28 m, one featuring diagonally configured BRBs and the other with superX configured BRBs. The first storey is 4.5 m tall, and all subsequent storeys are 3.6 m tall in both buildings, resulting in a total height of 15.3 m. The BRBF bays along both the X and Y directions are 4 m wide in the diagonally configured BRBF building, while they are 8 m wide in the superX configured BRBF building. These decisions were made to study the influence of gusset plate design on the brace configuration while ensuring a similar brace length and inclination in both buildings.

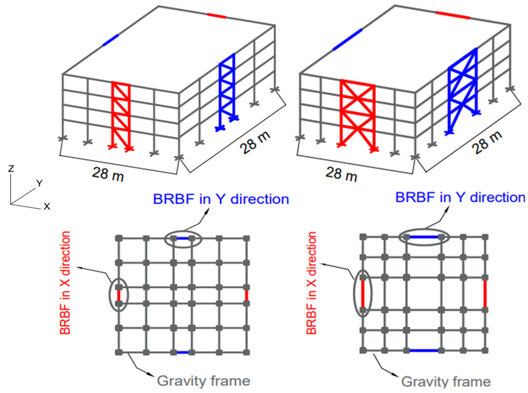

Figure 3: Schematic of the two case-study BRBF buildings with diagonal and superX configurations.

The equivalent static method and accidental eccentricity requirements from NZS 1170.5 were used to determine the lateral force distribution on the BRBFs. The member sizes in the diagonally configured BRBF building had to be significantly larger than those in the superX configured BRBF building. This difference arises because the diagonally configured BRBF building has only one brace per storey, while the superX configured BRBF building incorporates two braces per storey. Larger brace sizes require larger BRBF column and beam sizes in the diagonally configured BRBF building due to capacity design requirements. Design details and the final BRBF member sizes of both BRBF buildings are summarised in Table 1. The gusset plates of both buildings were sized using the NZS-3404 method, and the obtained gusset plate thicknesses are also summarised in Table 1.

NONLINEAR MODELLING OF THE CASE-STUDY BRBF BUILDINGS

3D models of the case-study BRBF buildings were developed in OpenSees [15] and the schematic of the superX configured BRBF is shown in Figure 4. The modelling process of the superX configured BRBF is discussed below, and the same procedure was used to model the diagonally configured BRBF. This process was previously developed by Sistla *et al.* [16] and later improved by Sistla *et al.* [8] to explicitly capture the out-of-plane buckling instability in BRBF buildings when subjected to bidirectional ground motions.

Elastic beam-column elements with concentrated plastic hinges at both ends were used to model the BRBF columns. The column bases were fixed, and the connection flexibility was ignored. The beams were modelled using elastic beam-column elements with pinned connections. The Ibarra-Medina-Krawinkler model [17] was adopted to represent the hysteretic behaviour of the plastic hinges in the beams and columns.

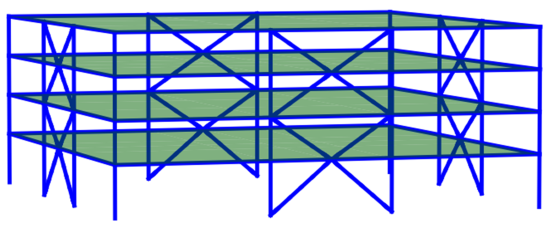

Figure 4: Schematic of the superX configured BRBF numerical model developed in OpenSees.

Table 1: Design summary of the case-study BRBF buildings.

Method of analysis	Equivalent static
Soil type	D
Importance level	2
Hazard factor (Z)	0.3 (Christchurch)
Ductility factor (μ)	4
Structural performance factor (S_p)	0.7
Design intensity	10 % probability of exceedance in 50 years
Seismic weight	Roof: 4658 kN Remaining floors: 5303 kN
Total seismic weight	20 567 kN
Horizontal design action coefficient (C_d)	0.11
Fundamental period (T_1)	Diagonal BRBF: 1 s SuperX BRBF: 0.87 s
Peak storey drift ratio at the design intensity	Diagonal BRBF: 1.65 % SuperX BRBF: 1.25 %
Summary of the final member sizes of the diagonally configured BRBF building	
Member	**Section**
Column (storeys 1–4)	400 WC 303.0
Beam (floors 1–4)	460 UB 67.1
Gravity column (storeys 1–2)	150 UC 37.2
Gravity column (storeys 3–4)	150 UC 23.4
Brace core and gusset plate (storey 1)	200 mm × 30 mm; 600 mm × 600 mm × 25 mm
Brace core and gusset plate (storey 2)	185 mm × 25 mm; 600 mm × 600 mm × 22 mm
Brace core and gusset plate (storey 3)	160 mm × 25 mm; 500 mm × 500 mm × 20 mm
Brace core and gusset plate (storey 4)	150 mm × 20 mm; 500 mm × 500 mm × 18 mm
Summary of the final member sizes of the SuperX-configured BRBF building	
Member	**Section**
Column (storeys 1–4)	400 WC 181.0
Beam (floors 1–4)	530 UB 92.4
Gravity column (storeys 1–2)	200 UC 46.2
Gravity column (storeys 3–4)	150 UC 23.4
Brace core and gusset plate (storey 1)	150 mm × 20 mm; 425 mm × 425 mm × 20 mm
Brace core and gusset plate (storey 2)	135 mm × 20 mm; 425 mm × 425 mm × 16 mm
Brace core and gusset plate (storey 3)	125 mm × 15 mm; 370 mm × 370 mm × 16 mm
Brace core and gusset plate (storey 4)	100 mm × 15 mm; 370 mm × 370 mm × 12 mm

The parameters of the hysteretic model were computed using the equations proposed by Lignos and Krawinkler [18] for beams and Lignos *et al.* [19] for columns. Geometric properties required for computing the plastic and post-capping rotation capacities of the frame members were obtained from [20]. Displacement-based fibre elements [21] were used to model the BRB cores, end zones, and gusset plates. The Zsarnóczay and Vigh steel material model was used to represent the constitutive behaviour of the brace core, and the model parameters were obtained from a previous study conducted by Zsarnóczay [22]. Their study validated the modelling approach against experimental tests; therefore, no further validation was carried out in the present study. The gusset plates were modelled as elements with equivalent uniform cross-sections, with out-of-plane geometric imperfections to simulate gusset plate buckling. Further details related to this equivalent uniform cross-section approach can be found in Sistla *et al.* [8].

The total gravity load was distributed proportionally to both the BRBF columns and the gravity columns, considering their respective tributary areas. The P-Δ geometric transformation with a large deformation assumption was adopted to capture the destabilising effects of the gravity loads. Leaning columns were modelled using elastic beam-column elements with plastic hinges and 1 % strain hardening. The slabs were modelled using shell elements with an elastic membrane section. Assuming composite slabs have negligible post-cracking bending stiffness, their out-of-plane moments were released. A mass and tangent stiffness proportional Rayleigh model was used with a 2 % damping ratio assigned to the first and third modes. It is acknowledged that the choice of damping model could introduce uncertainties in the estimated building response. Nonetheless, the damping model employed in this study is not anticipated to influence the conclusions of this study, which are based on the relative significance of gusset plate design on building performance.

The building IDs and fundamental periods of the two numerical models, featuring different brace configurations and gusset plates designed using the NZS-3404 method, are summarised in Table 2. The slight differences in fundamental periods, compared with those listed in Table 1, arise because the values in Table 2 are obtained from a detailed 3D nonlinear model, whereas those in Table 1 are from a 2D linear elastic model used at the design stage.

Table 2: Summary of nonlinear BRBF building models with gusset plates designed using the NZS-3404 method.

Configuration	ID	Fundamental period (T_1)
Diagonal	$D_{NZS-3404}$	0.944 s
SuperX	$S_{NZS-3404}$	0.862 s

SENSITIVITY OF OUT-OF-PLANE BUCKLING TO THE GUSSET PLATE DESIGN METHOD, BRACE CONFIGURATION, AND GUSSET PLATE LOCATION

Twenty bidirectional ground motion pairs at nine intensity levels were employed to conduct multiple stripe analysis [23] using the case-study BRBF building models summarised in Table 2. The ground motion set used in this study was previously selected by Yeow *et al.* [24] for Christchurch soil type D using the generalised conditional intensity measure approach by Bradley [25], with $S_a(1s)$ as the conditioning intensity measure. These ground motions are considered appropriate as the T_1 values of the building models are close to the conditioning period.

Buckling was mostly observed in the bottom two storeys of both models, followed by the top two storeys. For each gusset plate that experienced buckling, the gusset plate strength ratio was calculated. This ratio is defined as the peak brace compressive force obtained from nonlinear dynamic analysis, normalised by the gusset plate strength predicted by the design method. A strength ratio greater than 1 is considered conservative, whereas a value less than 1 indicates non-conservative behaviour. Histograms of the resulting strength ratio values obtained from the four different gusset plate design methods are illustrated in Figure 5.

An important observation from Figure 5a is that the NZS-3404 method exhibits non-conservative behaviour, as evidenced by an average median gusset plate strength ratio of 0.74 across both buildings. Although the gusset plates in the diagonally configured BRBF building are approximately 2.5 times more slender than those in the superX configuration, the median gusset plate strength ratios of the two buildings are nearly identical across all four design methods. Compared to the NZS-3404 method, the NZS-3404-revised method (Figure 5b) yields an

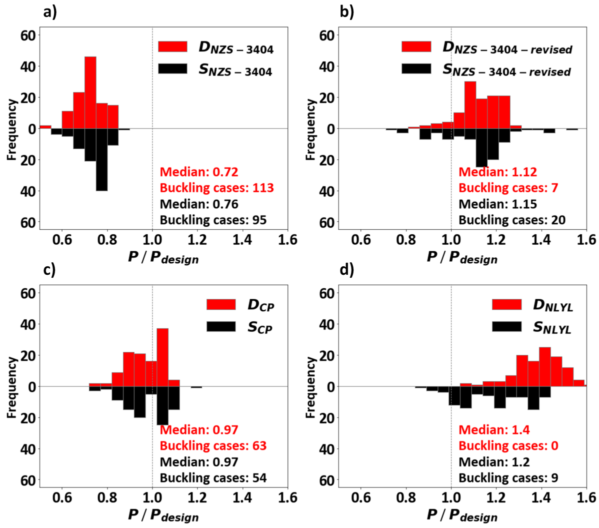

Figure 5: Histograms of the gusset plate strength ratios for diagonally and superX configured BRBFs, calculated using: a) NZS-3404, b) NZS-3404-revised, c) Cout-Patience (CP), and d) Notional load yield line (NLYL) methods. In the nomenclature A_B, A denotes the brace configuration — D for diagonal and S for superX — and B denotes the gusset plate design method.

average median strength ratio of 1.14 (53 % increase), the CP method (Figure 5c) 0.97 (31 % increase), and the NLYL method (Figure 5d) the highest at 1.3 (76 % increase). Correspondingly, the total number of gusset plate buckling cases is significantly reduced relative to the NZS-3404 method: to 27 cases with the NZS-3404-revised method (87 % reduction), 117 cases with the CP method (44 % reduction), and just 9 cases with the NLYL method (96 % reduction).

Histograms of the strength ratios of mid-span and corner gusset plates in the superX configured BRBFs, obtained using various gusset plate design methods, are illustrated in Figure 6. The results from the NZS-3404 method are shown in Figure 6a, the NZS-3404-revised method in Figure 6b, the CP method in Figure 6c, and the NLYL method in Figure 6d. None of the methods, except for the NLYL method, account for the lower capacity of the mid-span gusset plates compared to the corner gusset plates, as previously reported by Sistla *et al.* [8]. This trend is evident in the results, with the number of mid-span buckling cases being approximately 50 % higher than corner cases for the NZS-3404 and CP methods, and nearly 800 % higher for the NZS-3404-revised method. In contrast, the NLYL method shows a nearly equal number of buckling cases between mid-span and corner gusset plates.

As evident from Figures 5 and 6, the NLYL method is sufficiently conservative to mitigate gusset plate buckling in both case-study buildings, while also accounting for the reduced capacity of mid-span gusset plates. Therefore, this method is used to redesign the gusset plates in both buildings, and the revised gusset plate thicknesses are summarised in Table 3 below. Although the NLYL method results in different gusset plate thicknesses for mid-span and corner gusset plates in the superX BRBF building, to maintain a uniform gusset plate thickness across a storey, the thickness calculated for the mid-span gusset plates is also used for the corner gusset plates.

The building IDs and fundamental periods of two more numerical models, featuring different brace configurations and gusset plates designed using the NLYL method, are summarised in Table 4. These models are used to investigate the influence of gusset plate design on the global seismic performance and collapse risk of the case-study buildings in the following sections.

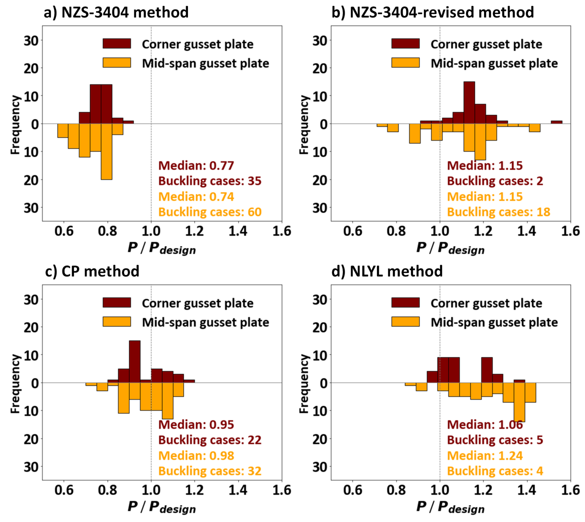

Figure 6: Histograms of the strength ratios of mid-span and corner gusset plates in the superX configured BRBFs, calculated using: a) NZS-3404, b) NZS-3404-revised, c) Cout-Patience (CP), and d) Notional load yield line (NLYL) methods.

Table 3: Storey-wise gusset plate thickness (T_{gp} in mm) calculated using the notional load yield line (NLYL) design method.

Brace configuration	Storey 1	Storey 2	Storey 3	Storey 4
Diagonal	36	32	28	25
SuperX	25	22	20	16

Table 4: Summary of nonlinear BRBF building models with gusset plates designed using the notional load yield line (NLYL) method.

Configuration	ID	Fundamental period (T_1)
Diagonal	D_{NLYL}	0.938 s
SuperX	S_{NLYL}	0.859 s

INFLUENCE OF THE GUSSET PLATE DESIGN METHOD ON THE GLOBAL SEISMIC PERFORMANCE

The gusset plates of the superX and diagonally configured BRBF buildings were redesigned using the NLYL method (Table 3). Redesigning the gusset plates was able to mitigate buckling of the gusset plates in the BRBF building models. The peak storey drift ratio (PSDR) and peak floor acceleration (PFA) obtained from multiple stripe analysis at the design intensity level (10 % probability of exceedance (PoE) in 50 years) for the models $D_{NZS-3404}$, $S_{NZS-3404}$, D_{NLYL}, and S_{NLYL} are compared in Figure 7.

The PSDR and PFA profiles at the design intensity level for the two buildings with gusset plates designed using the NZS-3404 and NLYL methods are depicted in Figure 7a and Figure 7b, respectively. It is worth noting that gusset plate buckling was only observed at intensity levels exceeding the 2 % PoE in 50 years; therefore, the choice of gusset plate design method had minimal influence on the structural response observed at this intensity level. In terms of brace configuration, although both configurations were designed with the same base shear

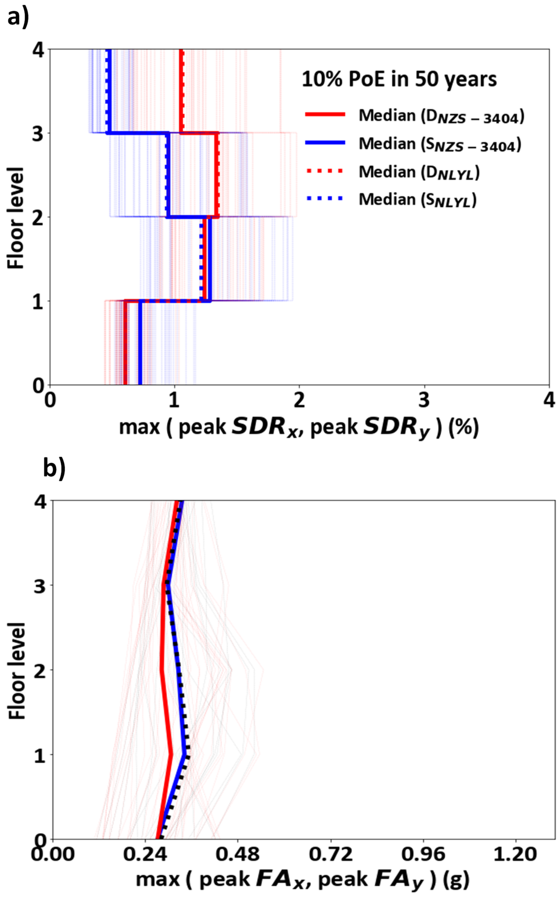

Figure 7: Design intensity level response of the two BRBF buildings with gusset plates designed according to the NZ 3404 method ($D_{NZS-3404}$ and $S_{NZS-3404}$), and the CP method (D_{NLYL} and S_{NLYL}): a) peak storey drift ratio profile, and b) peak floor acceleration.

coefficient, the diagonally configured BRBF building exhibited relatively greater flexibility (as indicated by T_1 values in Table 2) compared to the superX configured BRBF building. This difference is also evident in the median PSDR plots shown in Figure 7.

The median PSDR of the diagonally configured BRBF building at storey 4 is almost 50 % larger, while the PFAs are the same when compared to the superX configured BRBF building. Larger drifts in the upper storeys of the diagonally configured BRBF building can be attributed to the lower overturning resistance due to the reduced distance between the BRBF columns when compared to that of the superX configured BRBF building. For the brace angle considered in this study, the superX configuration may offer better performance compared to the diagonal configuration up to the design intensity level. While the superX configuration could be more expensive due to the increased number of connections, single diagonal BRBs carry the entire demand in either tension or compression, which may require larger foundations. By sharing the load between two braces in both tension and compression, superX-configured BRBs reduce foundation and connection demands. In practice, a cost analysis may be needed to select the optimal configuration, considering the effects on framing members, connections, and foundations.

The behaviour beyond the design intensity level, however, is expected to be different as the BRBF columns tend to have higher participation due to the yielding in BRBs. The diagonally configured BRBF building had only one BRB per storey, resulting in significantly larger BRBF columns compared to the superX configured BRBF building, due to the capacity design rules. Consequently, it is expected that the maximum PSDR over the building height in the diagonally configured BRBF building will be lower or equal to that of the superX configured BRBF building at higher intensities. This trend was observed in D_{NLYL} and S_{NLYL}, but not in $D_{NZS-3404}$ and $S_{NZS-3404}$, as illustrated in Figure 8a. This might be due to the presence of only one BRB in the diagonally configured building. SuperX configured BRBF typically has one brace in tension and the other in compression, leading to redundancy when the gusset plates in the compression BRB buckle. On the other hand, buckling of gusset plates in the diagonally configured BRBF implies a drop in resistance from the BRB, leading to increased PSDR and peak residual storey drift ratio, as observed in Figures 8a and 8b, respectively.

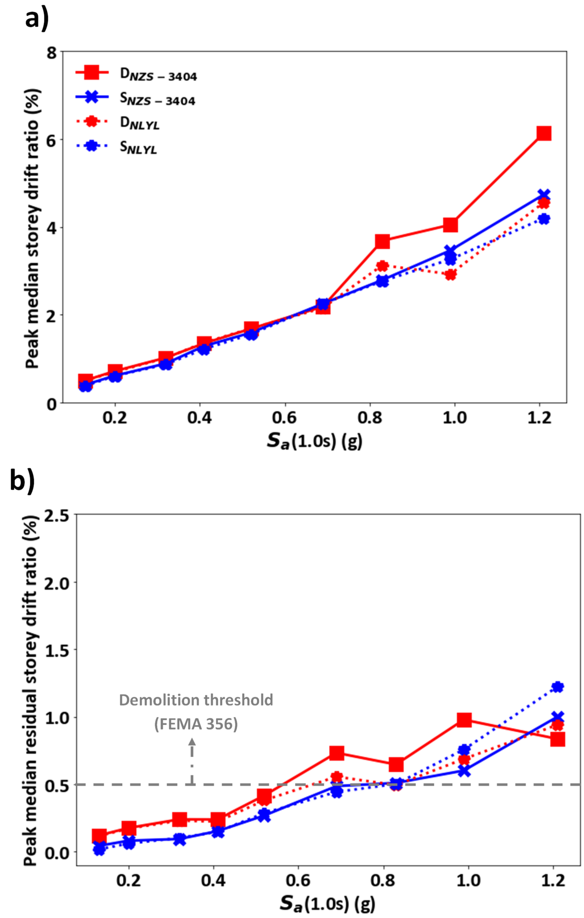

Figure 8: EDPs conditioned on non-collapse, along the building height of different BRBF models obtained across various ground motion intensity levels: a) maximum of median peak storey drift ratio, and b) maximum of median residual storey drift ratio.

Several studies recommend a residual SDR limit of 0.5 % as a threshold to consider building demolition, as it signifies potential damage beyond feasible repair [e.g., 24]. It is noteworthy that, regardless of the model being evaluated, building demolition is unlikely to be required after an earthquake shaking at the design intensity level. An interesting observation is that, irrespective of the gusset plate design, the probability of building demolition is considerably higher (occurring at lower shaking intensities) for BRBFs with a diagonal brace configuration as compared to the superX configuration. Some inconsistencies in the residual storey drift ratio trend can be seen in Figure 8b, and this arises due to a higher number of ground motions leading to collapse in the $D_{NZS-3404}$ and $S_{NZS-3404}$ models at the highest intensity level, distorting peak residual storey drift ratio statistics under non-collapse conditions.

INFLUENCE OF GUSSET PLATE DESIGN ON THE COLLAPSE RISK

The collapse fragility curves of the two buildings with gusset plates designed according to the NZS-3404 and NLYL methods, along with the seismic hazard curve, are illustrated in Figure 9. Modelling uncertainty was incorporated into the lognormal standard deviation of the collapse fragility curves using the square root sum of squares method, leaving the median unchanged. A value of 0.45 was chosen to represent the modelling uncertainty based on the recommendations of Liel *et al.* [26]. A summary of the collapse fragility curve parameters obtained from different building models is provided in Table 5.

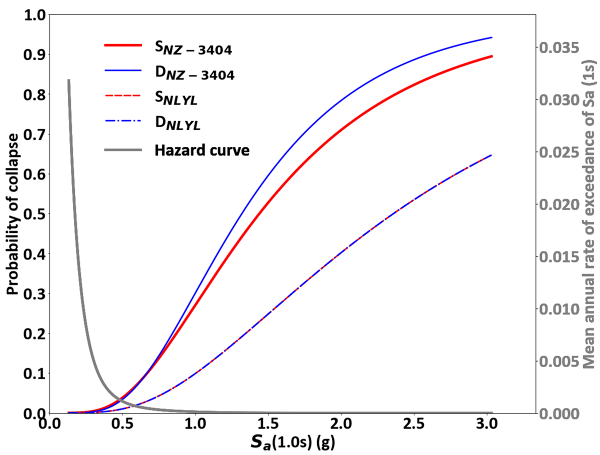

Figure 9: Comparison of collapse fragility curves of the case-study BRBF buildings with gusset plates designed using the NZS-3404 method and the NLYL method.

Table 5: Collapse fragility parameters and the estimated mean annual frequency of collapse (λ_c). θ is the median collapse capacity and β_T is the total uncertainty.

Model	θ (g)	β_T	λ_c
$D_{NZS-3404}$	1.32	0.53	20.0×10^{-5}
$S_{NZS-3404}$	1.44	0.59	18.7×10^{-5}
D_{NLYL}	2.32	0.66	6.00×10^{-5}
S_{NLYL}	2.32	0.63	6.00×10^{-5}

The median collapse capacities (θ) obtained from $D_{NZS-3404}$ and $S_{NZS-3404}$ are similar, with values of 1.32 g and 1.44 g, respectively. Meanwhile, the θ of the buildings with improved gusset plate design (D_{NLYL} and S_{NLYL}) is the same, with a value of 2.32 g. Improving the gusset plate design was able to mitigate gusset plate buckling and resulted in almost a 62 % and a 75 % increase in the θ of the diagonal and superX configured BRBF buildings, respectively. Gusset plate buckling is observed at relatively higher intensities, primarily affecting the collapse risk (mean annual frequency of collapse), and is not expected to significantly impact the expected annual loss. Nonetheless, gusset plate buckling is still expected to significantly affect the scenario-based losses at higher intensities. Both the case-study buildings with improved gusset plate design have satisfied the maximum code-based λ_c limit of 10^{-4}, while the buildings with gusset plates designed using the NZS-3404 method failed to do so.

CONCLUSION

The impact of gusset plate design on collapse risk was assessed by studying the performance of two BRBF buildings with diagonal and superX brace configurations. BRB gusset plates were initially designed following the NZS-3404 method, which is typically adopted in New Zealand. Multiple stripe analyses were then conducted using nonlinear BRBF models capable of simulating gusset plate buckling. In practice, gusset plates should be designed for the expected deformation demand, taken as the greater of 2 % storey drift or twice the design storey drift, as per ANSI/AISC 341-22. Using the NZS-3404 method, buckling of the gusset plates was observed in both models beyond the 2 % PoE in the 50-year intensity level. The performance of each gusset plate design method was assessed using the strength ratio, defined as the peak brace force normalised by the design gusset plate strength, for gusset plates that experienced buckling. The NZS-3404 gusset plate design method was found to be non-conservative, with a median strength ratio of 0.76 for the superX configured BRBF and 0.72 for the diagonally configured BRBF. The susceptibility of gusset plate buckling was not found to exhibit sensitivity to the brace configuration (diagonal vs. superX). Notably, mid-span gusset plates in $S_{NZS-3404}$ displayed lower resistance to buckling, making them more susceptible compared to corner gusset plates.

The gusset plate strength ratio values of both buildings were re-evaluated using three alternative approaches: the NZS-3404-revised method, the Court-Patience method, and the notional load yield line method. The NZS-3404-revised and Court-Patience methods are characterised as conservative, on average, since the median strength ratio values from these methods were close to or above 1. In contrast, the notional load yield line method, which explicitly accounts for both the gusset plate location and the influence of out-of-plane drifts, emerged as the best option, with a median strength ratio value of 1.3, on average.

The notional load yield line method was applied to redesign the gusset plates in both BRBF buildings, followed by a repetition of the multiple stripe analysis to assess the enhancement in global seismic BRBF performance of the diagonal and superX configured BRBF buildings. This method effectively mitigated gusset plate buckling, with no failure instances observed up to an intensity level corresponding to 0.2 % PoE in 50 years. The collapse risk was reduced by a factor of about 3.5 in both building models due to this revision in the gusset plate design. The BRBFs with gusset plates designed using the NZS-3404 method did not meet the code-specified collapse risk limit of 10^{-4}, whereas those designed using the notional load yield line method did. It is important to note that the cost implications of adopting a more conservative gusset plate design are not expected to be significant. In this study, the gusset plate thickness increased by 30 %, on average, when the design was revised using the notional load yield line method.

REFERENCES

1 Bruneau M and MacRae G (2019). "Building Structural Systems in Christchurch's Post-Earthquake Reconstruction". *Earthquake Spectra*, **35**(4): 1953–1978. https://doi.org/10.1193/052818EQS126O

2 ANSI/AISC 341-22 (2022). *Seismic Provisions for Structural Steel Buildings*. 341-22, American Institute of Steel Construction, Chicago, IL.

3 Vazquez-Colunga SY, Lee CL and MacRae GA (2021). "Bidirectional loading performance of gusset plates in buckling-restrained braced frames". *Engineering Structures*, **242**: 112521. https://doi.org/10.1016/j.engstruct.2021.

112521

4 Westeneng BA (2016). *"Buckling behaviour of gusset plates in buckling-restrained braced frames"*. Master's Thesis, University of Canterbury.

5 Song Y, Zhang M, Ke K, Yam MC and Lin XM (2023). "Behaviour and design of gusset plates in steel structures: A state-of-the-art review". *Journal of Constructional Steel Research*, **211**: 108188. https://doi.org/10.1016/j.jcsr.2023.108188

6 Khoo HH, Tsai KC, Tsai CY, Tsai CY and Wang KJ (2016). "Bidirectional substructure pseudo-dynamic tests and analysis of a full-scale two-story buckling-restrained braced frame". *Earthquake Engineering & Structural Dynamics*, **45**(7): 1085–1107. https://doi.org/10.1002/eqe.2696

7 Court-Patience D and Garnich M (2021). "Buckling analysis of gusset plates with bolted connections using finite element modeling". *Journal of Constructional Steel Research*, **176**: 106420. https://doi.org/10.1016/j.jcsr.2020.106420

8 Sistla S, Chandramohan R and Sullivan TJ (2025). "A Macro-Model for Simulating Gusset Plate Buckling in Buckling-Restrained Braced Frame Buildings". *Earthquake Engineering & Structural Dynamics*. https://onlinelibrary.wiley.com/doi/10.1002/eqe.4383

9 Thornton WA (1984). "Bracing connections for heavy construction". *Engineering Journal*, **21**(3): 139–148.

10 AISC-341 (2010). *Seismic Design Provisions for Steel Structures*. American Institute of Steel Construction (AISC), Chicago, IL.

11 Chou CC, Liu JH and Pham DH (2012). "Steel buckling-restrained braced frames with single and dual corner gusset connections: seismic tests and analyses". *Earthquake Engineering & Structural Dynamics*, **41**(7): 1137–1156. https://doi.org/10.1002/eqe.1176

12 Dong W (2021). *"Seismic performance of glulam frames with buckling restrained braces (BRBs)."* Ph.D. Thesis, University of Canterbury.

13 Zaboli B, Clifton G and Cowie K (2017). "Out-of-plane stability of gusset plates using a simplified notional load yield line method". *Proceedings of the NZSEE Annual Conference 2017, Christchurch, New Zealand*.

14 Takeuchi T, Ozaki H, Matsui R and Sutcu F (2014). "Out-of-plane stability of buckling-restrained braces including moment transfer capacity". *Earthquake Engineering & Structural Dynamics*, **43**(6): 851–869. https://doi.org/10.1002/eqe.2376

15 Zhu M, McKenna F and Scott MH (2018). "OpenSeesPy: Python library for the OpenSees finite element framework". *SoftwareX*, **7**: 6–11.

16 Sistla S, Chandramohan R and Sullivan TJ (2022). "Modelling the out-of-plane buckling behaviour of BRBFs". *New Zealand Society for Earthquake Engineering*.

17 Ibarra LF, Medina RA and Krawinkler H (2005). "Hysteretic models that incorporate strength and stiffness deterioration". *Earthquake engineering & structural dynamics*, **34**(12): 1489–1511. https://doi.org/10.1002/eqe.495

18 Lignos DG and Krawinkler H (2011). "Deterioration modeling of steel components in support of collapse prediction of steel moment frames under earthquake loading". *Journal of Structural Engineering*, **137**(11): 1291–1302. https://doi.org/10.1061/(ASCE)ST.1943-541X.0000376

19 Lignos DG, Hartloper AR, Elkady A, Deierlein GG and Hamburger R (2019). "Proposed updates to the ASCE 41 nonlinear modeling parameters for wide-flange steel columns in support of performance-based seismic engineering". *Journal of Structural Engineering*, **145**(9): 04019083. https://doi.org/10.1061/(ASCE)ST.1943-541X.0002353

20 Liberty Steel (2014). *Hot rolled and structural steel products*. Liberty Primary Steel manufactures.

21 Neuenhofer A and Filippou FC (1997). "Evaluation of nonlinear frame finite-element models". *Journal of structural engineering*, **123**(7): 958–966. https://doi.org/10.1061/(ASCE)0733-9445(1997)123:7(958)

22 Zsarnóczay Á (2013). *"Experimental and numerical investigation of buckling-restrained braced frames for Eurocode conform design procedure development"*. Ph.D. Thesis, Budapest University of Technology and Economics (Hungary).

23 Jalayer F (2003). *"Direct probabilistic seismic analysis: implementing non-linear dynamic assessments"*. Ph.D. Thesis, Stanford University.

24 Yeow T, Orumiyehei A, Sullivan T, MacRae G, Clifton G and Elwood K (2018). "Seismic performance of steel friction connections considering direct-repair costs". *Bulletin of Earthquake Engineering*, **16**: 5963–5993.

25 Bradley BA (2010). "A generalized conditional intensity measure approach and holistic ground-motion selection". *Earthquake Engineering & Structural Dynamics*, **39**(12): 1321–1342. https://doi.org/10.1002/eqe.995

26 Liel AB, Haselton CB, Deierlein GG and Baker JW (2009). "Incorporating modeling uncertainties in the assessment of seismic collapse risk of buildings". *Structural Safety*, **31**(2): 197–211. https://doi.org/10.1016/j.strusafe.2008.06.002